Electronic Supplementary Material (ESI) for Materials Horizons.

Supporting Information: Optical Phonons in Methylammonium Lead Halide Perovskites and Implications for Charge Transport

Michael Sendner[†‡], Pabitra K. Nayak[⊥], David Egger[§], Sebastian Beck, Christian Müller[†‡+], Bernd Epding[†‡+], Wolfgang Kowalsky[†‡+], Leeor Kronik[§], Henry J. Snaith[⊥], Annemarie Pucci[†‡‖], and Robert Lovrincic[‡+]*

[†]InnovationLab, Speyerer Str. 4, 69115 Heidelberg, Germany

[‡]Kirchhoff-Institute for Physics, Universität Heidelberg, INF 227, 69120 Heidelberg, Germany

[⊥]Clarendon Laboratory, Department of Physics, University of Oxford, Oxford OX1 3PU, UK

[§]Department of Materials and Interfaces, Weizmann Institute of Science, Rehovoth 76100, Israel

[+]Institute for High frequency Technology, TU Braunschweig, Schleinitzstr. 22, 38106 Braunschweig, Germany

[‖]Centre for Advanced Materials, Universität Heidelberg, INF 225, 69120 Heidelberg, Germany

1. Comparison with Lorentzian model fitting

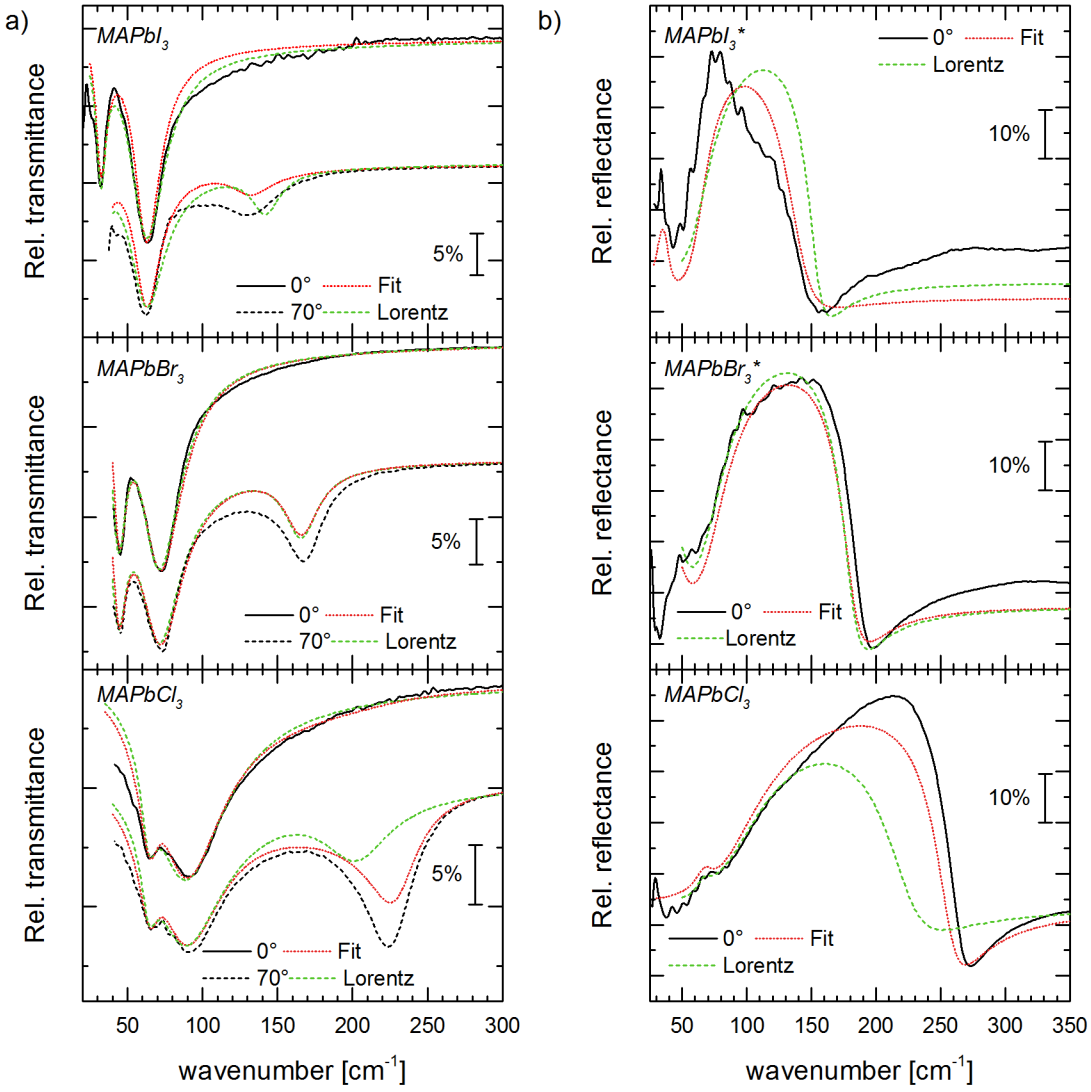

Figure S1. a) Relative transmittance of a 266 nm thick $CH_3NH_3PbI_3$ (top), 287 nm thick $CH_3NH_3PbBr_3$ (middle) and 226 nm $CH_3NH_3PbCl_3$ (bottom) thin film on a silicon substrate under normal incidence (solid) an under 70° angle of incidence (dashed) with unpolarized light. Gervais model fit for both angle of incidences for every $MAPbX_3$ thin films is shown in red dashed lines, Lorentzian model fitting is shown in green dashed lines. b) Relative reflectance spectra of $MAPbI_3$ (top), $MAPbBr_3$ (middle) and $MAPbCl_3$ (bottom) single crystals at room temperature with unpolarized light under 80° angle of incidence (gold mirror as reference). (Spectra with star were scaled in intensity). Shown are also the calculated reflectance spectra from the corresponding thin film model for the Gervais model (red dashed lines) and Lorentzian model fit (green dashed lines).

For the fitting of a Lorentzian model, the dielectric function

$$\varepsilon(\omega) = \varepsilon_\infty + \sum_i \frac{A_i^2}{\omega_{\mathrm{TO}}^2 - \omega^2 - \mathrm{i}\gamma\omega}$$

with the resonance frequency of the TO mode ω_{TO}, its damping γ and amplitude A were used. The dielectric functions sums up over all vibrational modes and also accounts for the dielectric background taken from mid infrared data[1]. Both angles of incidence were simultaneously fitted for one material resulting in the green dashed lines in Fig. S1

2. Fit with additional central peak

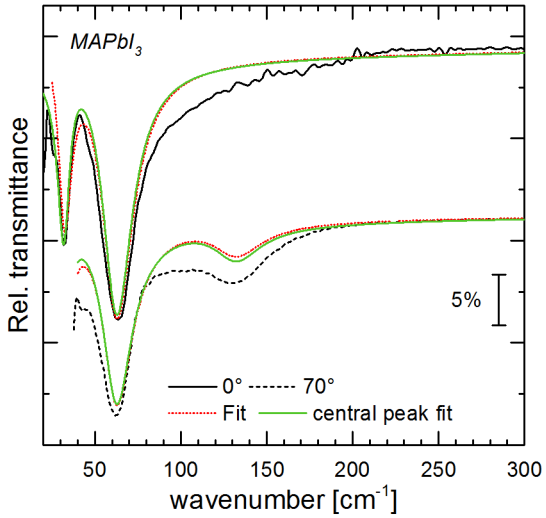

Figure S2. Relative transmittance of a 266 nm thick $CH_3NH_3PbI_3$ thin film on a silicon substrate under normal incidence (solid) an under 70° angle of incidence (dashed) with unpolarized light. Gervais model fit for both angle of incidences for $MAPbI_3$ is shown in red dashed lines, fitting with an additional central peak is shown in green. The parameters of this fit can found in table S1.

Table S1. Summary of the obtained TO and LO phonon frequencies and dampings with an additional oscillator in the model.

	ω_{TO} [cm^{-1}]	γ_{TO} [cm^{-1}]	ω_{LO} [cm^{-1}]	γ_{LO} [cm^{-1}]
	15	130.6	34	131.5
$MAPbI_3$	32	7.9	40	8.0
	63	18.0	133	31.8

3. AFM measurements

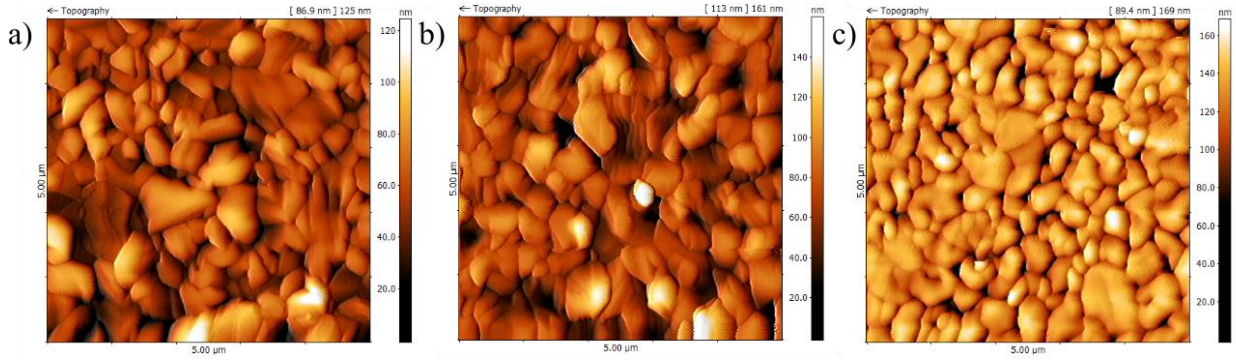

Figure S3. AFM measurements of $MAPbX_3$ thin films on a silicon substrate. a) $MAPbI_3$, b) $MAPbBr_3$ c) $MAPbCl_3$. All three thin films were fabricated using a vapor assisted evaporation process.

4. Calculated complex conductivity

We calculated the complex conductivity $\sigma = \sigma_1 + \mathrm{i}\sigma_2 = \omega\varepsilon_0(\varepsilon_2 + \mathrm{i}(1 - \varepsilon_1))$ with the determined dielectric function of the thin films. The peak positions are quite comparable to the data published[2] by La-o-vorakiat et al. for $MAPbI_3$ but deviate in the σ_1 amplitude (and thereby in the oscillator strength) by a factor of approx. 2.

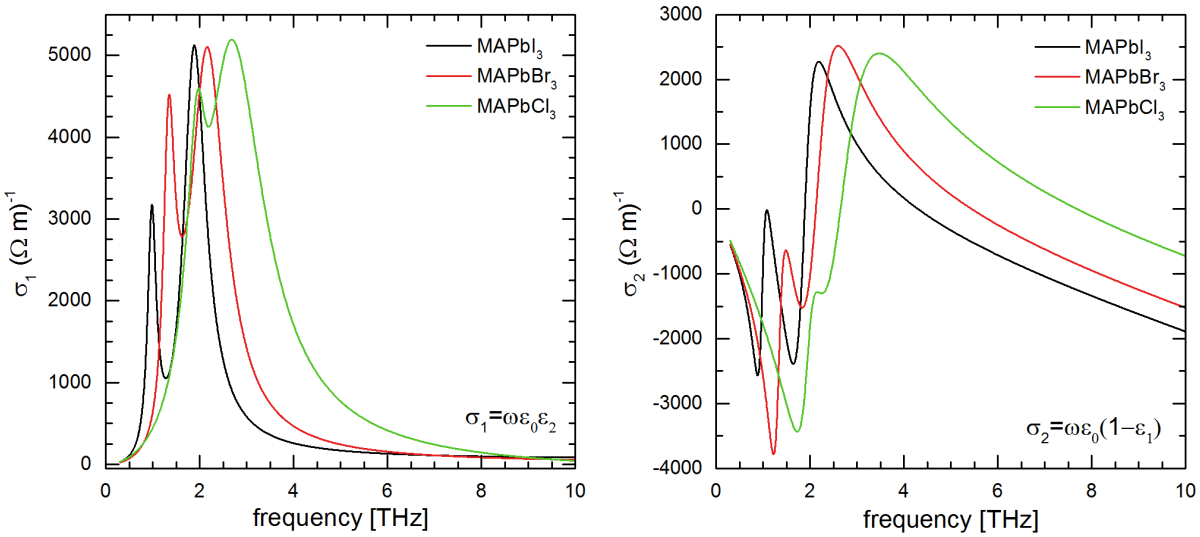

Figure S4. Calculated complex conductivity $\sigma = \sigma_1 + i\sigma_2$ for the three halide perovskites. a) Real part of the conductivity $\sigma_1 = \omega\varepsilon_0\varepsilon_2$ and b) imaginary part of the conductivity $\sigma_2 = \omega\varepsilon_0(1 - \varepsilon_1)$.

5. Images of the used $MAPbX_3$ single crystals

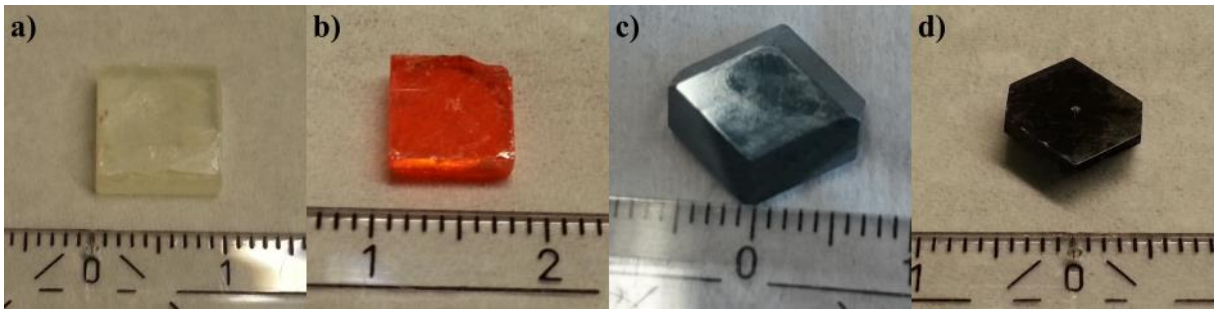

Figure S5. Pictures of the used $MAPbX_3$ single crystals. a) $MAPbCl_3$. b) $MAPbBr_3$. c) $MAPbI_3$ from the top and d) from the bottom.

6. Determination of the single phonon frequency

To calculate a single phonon frequency from our modeled data, we followed the ansatz of Hellwarth and Biaggio (Ref. (3)). The oscillator strength W_i of the LO phonon modes is calculated with help of the LO-TO-splitting via

$$W_i^2 = \frac{1}{\varepsilon_\infty}\left(\omega_{\mathrm{LO},i}^2 - \omega_{\mathrm{TO},i}^2\right)$$

with subsequent quadratic mean ($W^2 = \sum {W_i}^2$) over the two single oscillator strength to obtain the oscillator strength of the single phonon branch W. The frequency ω_{LO} (in wavenumbers) of this branch is then found by solving

$$\frac{W^2}{\omega_{\mathrm{LO}}}\coth\left(\frac{hc\omega_{\mathrm{LO}}}{2k_{\mathrm{B}}T}\right) = \sum_{i=1}^{2}\frac{W_i^2}{\omega_{\mathrm{LO},i}}\coth\left(\frac{hc\omega_{\mathrm{LO},i}}{2k_{\mathrm{B}}T}\right).$$

7. Minimization of the free polaron energy

For given values of the coupling constant α and temperature T ($\beta = h\omega_{\mathrm{LO}}/k_{\mathrm{B}}T$) we minimized the free energy of the polaron F by the following equations given in Ref. (3)

$$F = -(A + B + C)$$

with the contributions

$$A = \frac{3}{\beta}\left[\ln\left(\frac{v}{w}\right) - \frac{\ln(2\pi\beta)}{2} - \ln\frac{\sinh\left(\frac{v\beta}{2}\right)}{\sinh\left(\frac{w\beta}{2}\right)}\right]$$

$$B = \frac{\alpha v}{\sqrt{\pi}[\exp(\beta) - 1]}\int_0^{\beta/2}\frac{\exp(\beta - x) + \exp(x)}{\sqrt{w^2 x\left(1 - \frac{x}{\beta}\right) + Y(x)(v^2 - w^2)/v}}\,\mathrm{d}x$$

$$Y(x) = \frac{1}{1-\exp(-v\beta)}\{1+\exp(-v\beta)-\exp(-vx)-\exp(v[x-\beta])\}$$

$$C = \frac{3(v^2-w^2)}{4v}\left(\coth\left(\frac{v\beta}{2}\right)-\frac{2}{v\beta}\right)$$

to obtain the temperature dependent variational parameters *v* and *w*.

8. Calculation of mobility

Beside the already defined parameters in the main part, the equation for the mobility

$$\mu = \frac{3\sqrt{\pi}e}{2\pi\omega_{\mathrm{LO}}m_{\mathrm{e}}^{*}\alpha}\frac{\sinh(\beta/2)}{\beta^{5/2}}\frac{w^3}{v^3}\frac{1}{K}$$

contains the function *K* which is calculated (see Ref. (4) for further details) be the following equations which only depend on $\beta = h\omega_{\mathrm{LO}}/k_{\mathrm{B}}T$ and the variational parameters *v* and *w*:

$$K(a,b) = \int_0^{\infty} \frac{\cos(u)}{(u^2+a^2-b\cos(v\cdot u))^{3/2}}\,\mathrm{d}u,$$

$$a^2 = \left(\frac{\beta}{2}\right)^2 + R\beta\coth\left(\frac{\beta v}{2}\right),$$

$$b = \frac{R\beta}{\sinh\left(\frac{b\beta v}{2}\right)},$$

$$R = \frac{v^2-w^2}{w^2 v}.$$

9. Temperature dependence of the mobility

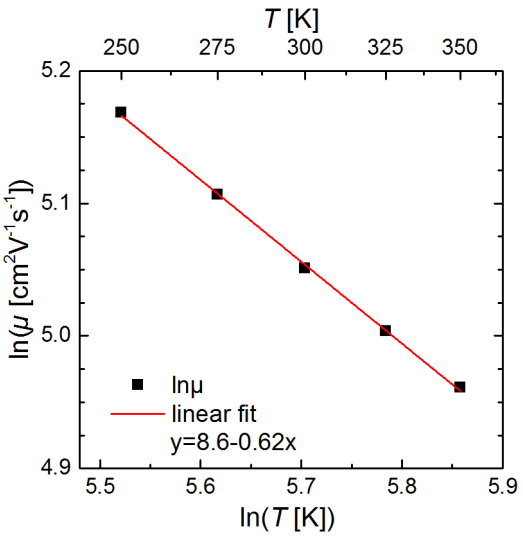

Figure S6. Calculated temperature dependence of the mobility of $MAPbBr_3$ using the equations described in the main part between 250 K and 350 K. With a linear fit we obtained a slope of -0.62 $\pm$ 0.01 and thus $\mu \propto T^{-0.62}$.

References:

(1) Glaser, T.; Müller, C.; Sendner, M.; Krekeler, C.; Semonin, O. E.; Hull, T. D.; Yaffe, O.; Owen, J. S.; Kowalsky, W.; Pucci, A.; Lovrinčić, R. *J. Phys. Chem. Lett.* **2015**, *6* (15), 2913–2918

(2) La-o-vorakiat, C.; Xia, H.; Kadro, J. M.; Salim, T.; Zhao, D.; Ahmed, T.; Lam, Y. M.; Zhu, J.-X.; Marcus, R. A.; Michel-Beyerle, M.-E.; Chia, E. E. *J. Phys. Chem. Lett*, **2015**, *7* (1), 1-6

(3) Hellwarth, R. W.; Biaggio, I. *Phys. Rev. B* **1999**, *60* (1), 299–307

(4) I. Biaggio, R. W. Hellwarth and J. P. Partanen, *Phys. Rev. Lett.*, 1997, **78**, 891–894